Supporting Information

for

Copper/α-Ketocarboxylate Chemistry With Supporting Peralkyated Diamines: Reactivity of Copper(I) Complexes and Dicopper-Oxygen Intermediates

Aalo K. Gupta and William B. Tolman*

Department of Chemistry and Center for Metals in Biocatalysis, University of Minnesota, 207 Pleasant St. SE, Minneapolis, MN 55455. E-mail: wtolman@umn.edu.

Contents

Table S1. X-ray crystallographic parameters for (tBu_2Me_2eda)Cu(BF), (tBu_2Me_2eda)Cu(*p-nitro*-BF), and (Me_4pda)$CuBF_2$. For a complete description, see the CIF.

	(tBu_2Me_2eda)Cu(BF)	(tBu_2Me_2eda)Cu(*p-nitro*-BF)	(Me_4pda)$CuBF_2$
Empirical formula	$C_{20}H_{33}CuN_2O_3$	$C_{20}H_{32}CuN_3O_5$	$C_{23}H_{28}CuN_2O_6$
Formula weight	413.02	458.03	492.01
Crystal system	Monoclinic	Monoclinic	Triclinic
Space group	P_{21}	$P_{21/c}$	P_{-1}
a (Å)	9.7882(6)	19.2670(13)	8.076(5)
b (Å)	10.3914(6)	8.9816(6)	11.998(5)
c (Å)	10.3951(7)	13.6990(9)	12.092(5)
α (deg)	90	90	86.948(5)
β (deg)	97.540(2)	107.274(2)	81.838(5)
γ (deg)	90	90	76.588(5)
Volume ($Å^3$)	1048.18(11)	2263.7(3)	1127.9(10)
Z	2	4	2
T(K)	173(2)	173(2)	173(2)
ρ (calculated) (Mg/m^3)	1.309	1.347	1.449
θ range (deg)	1.98 to 25.06	1.11 to 25.07	1.7 to 25.06
μ (mm^{-1})	1.062	0.999	1.010
Reflections collected	10469	21392	10940
Independent reflections	3708	4019	4007
parameters	244	313	293
R1, wR2 (for $I > 2\sigma(I)$)	0.0249, 0.0598	0.0660, 0.1425	0.0355, 0.0844
GOF	1.006	1.037	0.985
Largest Peak, Hole ($e.Å^{-3}$)	0.307 and -0.181	1.917 and -1.754	0.424 and -0.382
F(000)	440	972	514
Crystal color, morphology	yellow, plate	gold, plate	green, block
Crystal size	0.50 x 0.40 x 0.10 mm^3	0.50 x 0.40 x 0.10	0.4 x 0.3 x 0.2
Index ranges	$-11 \le h \le 11$, $-12 \le k \le 12$, $-12 \le l \le 12$	$-22 \le h \le 22$, $-10 \le k \le 10$, $-16 \le l \le 16$	$-9 \le h \le 9$, $-14 \le k \le 14$, $-14 \le l \le 14$

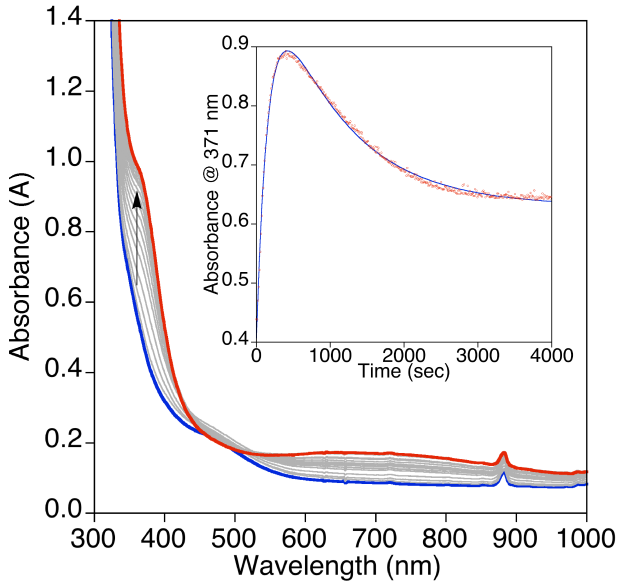

Figure S1. UV-vis spectral data for the reaction of (tBu_2Me_2eda)Cu(nitro-BF) in CH_2Cl_2 (0.67 mM) (*blue)* with O_2 at -80 °C with spectra shown every 20 sec (spectrum for the intermediate shown in *red*). The inset displays the time trace for the formation and decay of the intermediate data monitored at 375 nm (*red dots*) and fit to a bi-exponential equation [A_t = A1 – A2*exp(-k_1*t) + A3*exp(-k_2*t), k_1 = 0.0062 s^{-1} and k_2 = 0.0010 s^{-1}; R = 0.998].

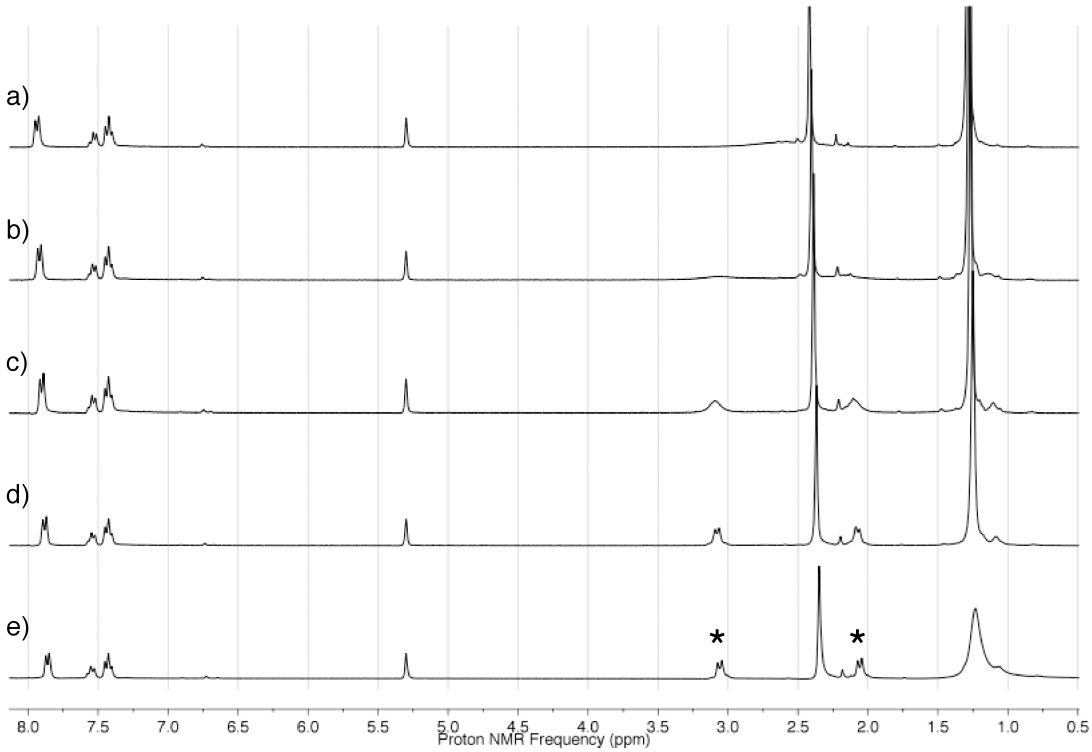

Figure S2. Variable temperature ^{1}H NMR spectra of (tBu_2Me_2eda)Cu(BF) in CD_2Cl_2 at a) Room temperature; b) 0 °C; c) –20 °C; d) –40 °C; e) –60 °C. The new features observed at –60 °C and modeled in Figures S3 and S4 are marked with asterisks.

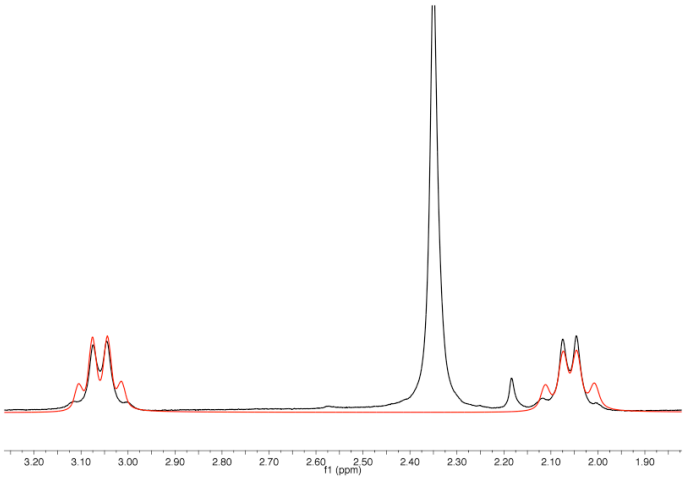

Figure S3. Expansion of the ^{1}H NMR features at ~2.06 and ~3.06 ppm for (tBu_2Me_2eda)Cu(BF) in CD_2Cl_2 at −60 °C (*black*) with a simulated spectrum overlaid (*red*). The simulated spectrum was generated with 4 spins (A, B, C, and D) with A = 2.09 ppm, B = 2.03 ppm, C= 3.09 ppm, and D = 3.03 ppm and $J_{AB} = J_{CD}$ = 15 Hz, $J_{AC} = J_{AD} = J_{BC} = J_{BD}$ = 3 Hz using MestReNova v6.0.2 NMR processing software.

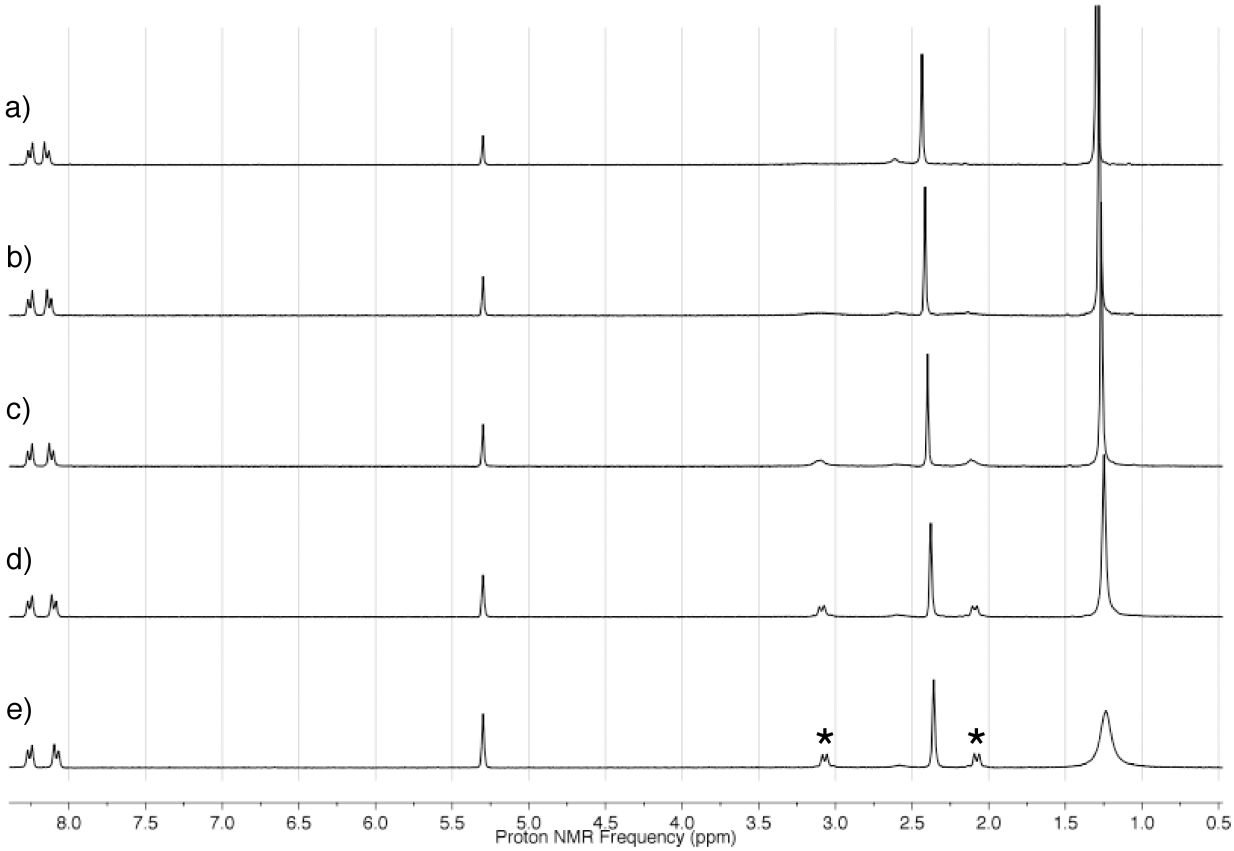

Figure S4. Variable temperature ^{1}H NMR spectra of (tBu_2Me_2eda)Cu(nitro-BF) in CD_2Cl_2 at a) Room temperature; b) 0 °C; c) −20 °C; d) −40 °C; e) −60 °C. The new features observed at −60 °C are marked with asterisks.

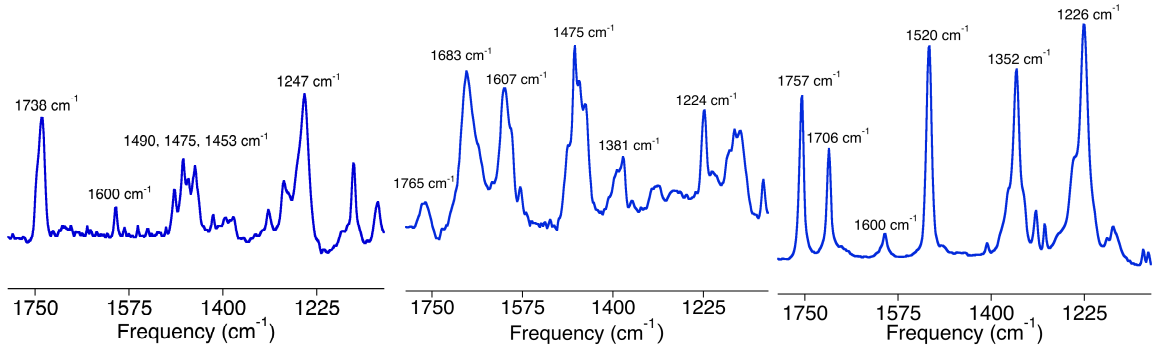

Figure S5. FTIR spectra of solid samples of Bu_4NBA (*left*), Bu_4NBF (*center*), and nitro-BF (free acid) (*right*).

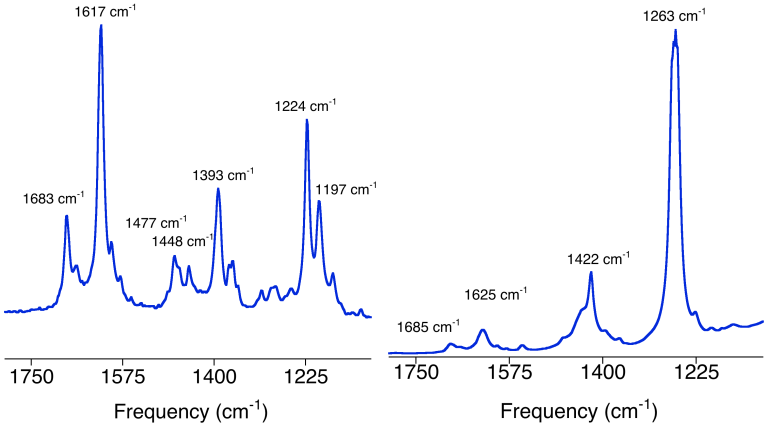

Figure S6. FTIR spectra of solid sample of $(tBu_2Me_2eda)Cu(BF)$ (*left*) and solution sample of $(tBu_2Me_2eda)Cu(BF)$ (10 mM in CH_2Cl_2) (*right*).

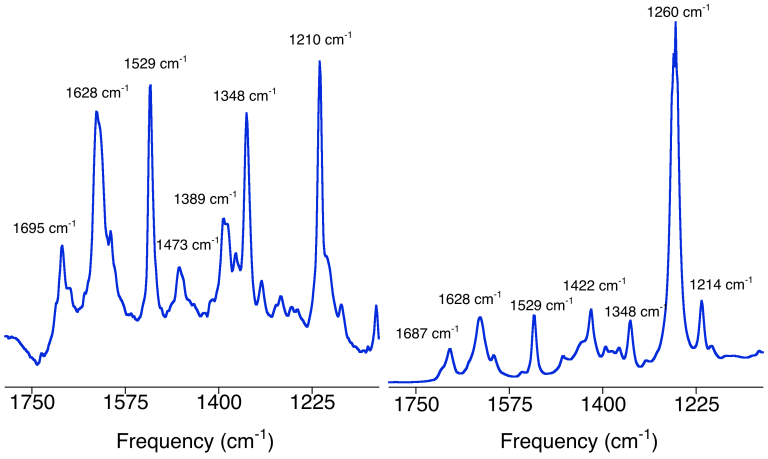

Figure S7. FTIR spectra of solid sample of $(tBu_2Me_2eda)Cu(nitro\text{-}BF)$ (*left*) and solution sample of $(tBu_2Me_2eda)Cu(nitro\text{-}BF)$ (10 mM in CH_2Cl_2) (*right*).

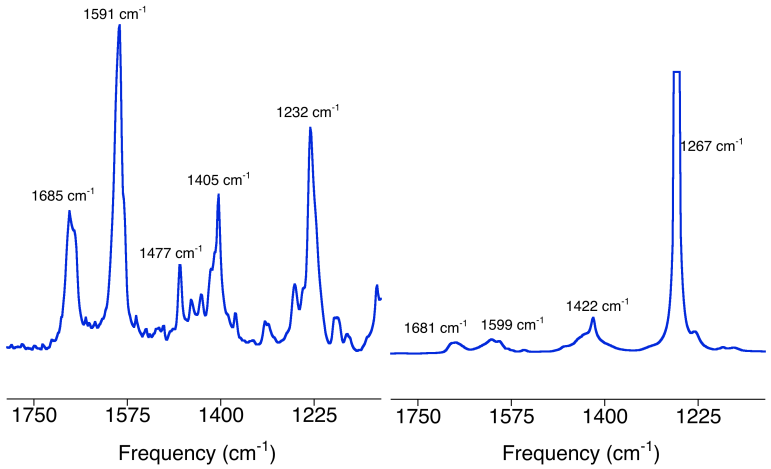

Figure S8. FTIR spectra of solid sample of $(Me_4pda)Cu(BF)_2$ (*left*) and solution sample of $(Me_4pda)Cu(BF)_2$ (10 mM in CH_2Cl_2) (*right*).

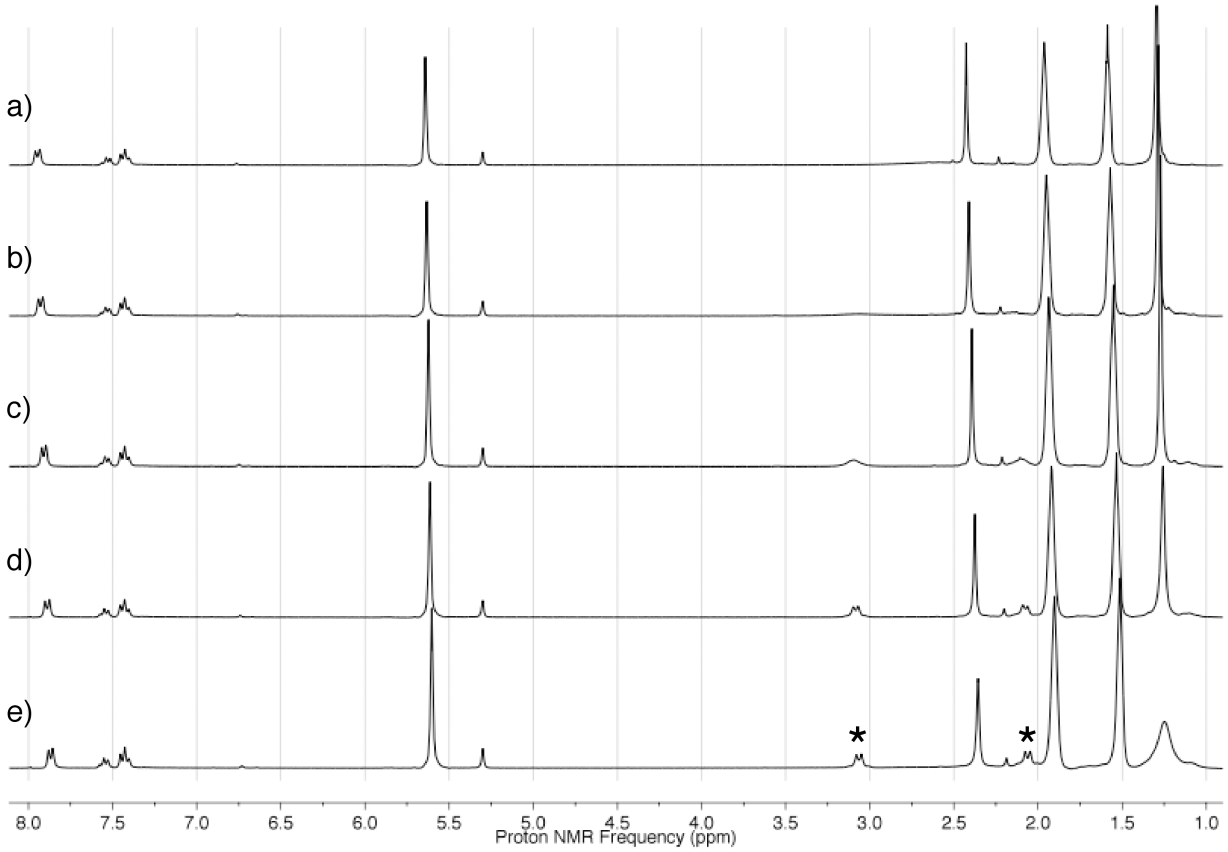

Figure S9. Variable temperature ^{1}H-NMR spectra of $(tBu_2Me_2eda)Cu(BF)$ in CD_2Cl_2 with 5 equivalents of cyclohexene at a) Room temperature; b) 0 °C; c) −20 °C; d) −40 °C; e) −60 °C. New features observed at −60 °C are marked with asterisks.

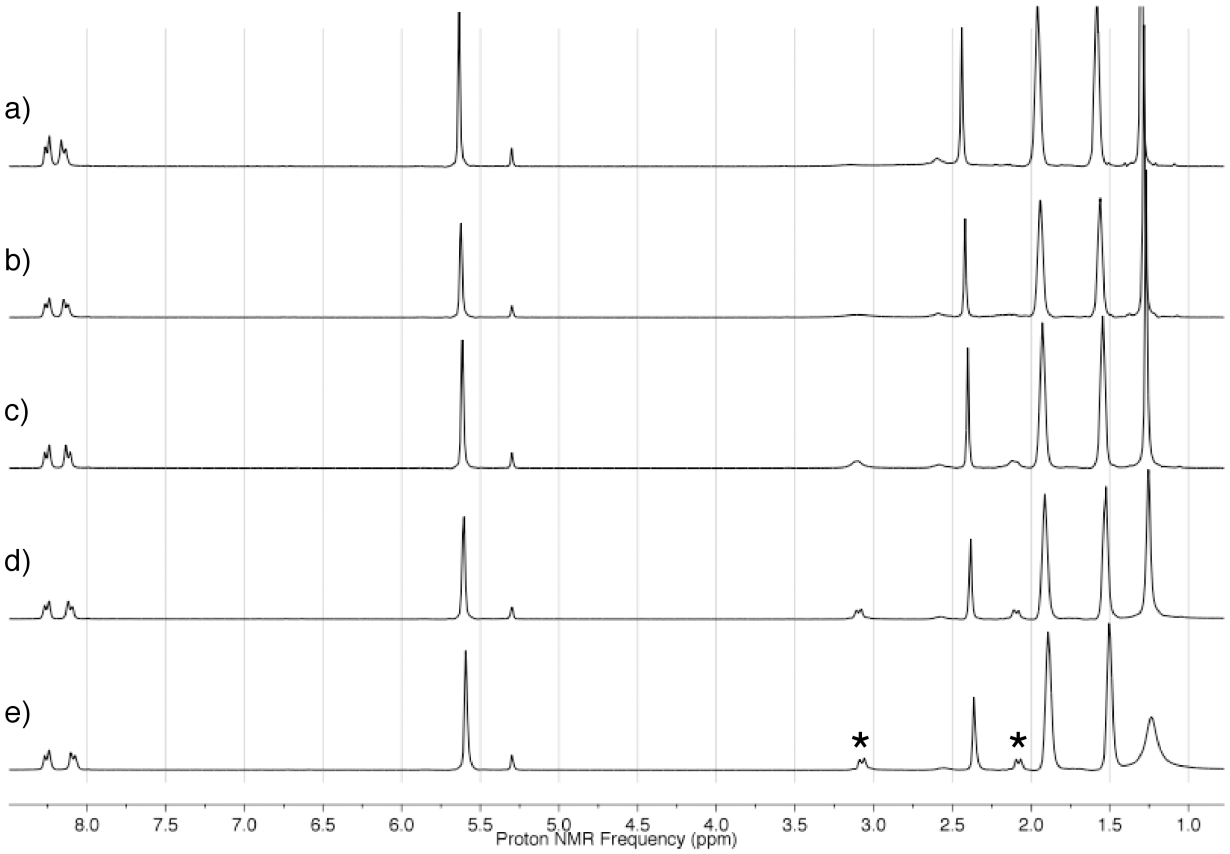

Figure S10. Variable temperature ^{1}H-NMR spectra of (tBu_2Me_2eda)Cu(nitro-BF) in CD_2Cl_2 with 5 equivalents of cyclohexene at a) Room temperature; b) 0 °C; c) −20 °C; d) −40 °C; e) −60 °C. New features observed at −60 °C are marked with asterisks.

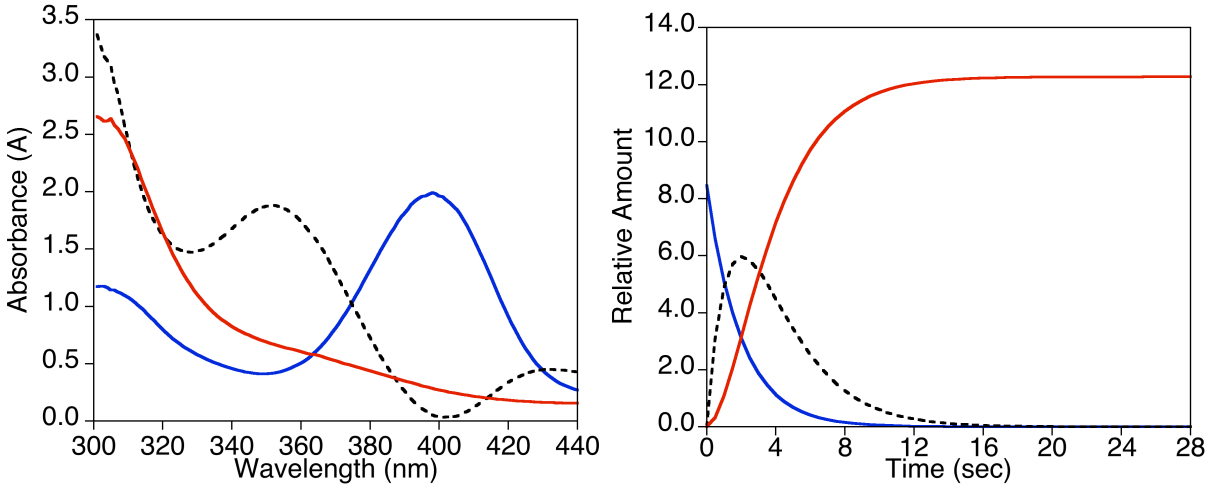

Figure S11. Results from the global fitting analysis of the UV-vis spectra obtained during the reaction of $[(Me_4pda)_2Cu_2O_2]OTf_2$ in CH_2Cl_2 (0.1 mM) at –80 ºC (*blue*) with 60 equivalents Bu_4NBF. Data was truncated to a region between 300-440 nm to only include areas of significant spectral change followed by singular value decomposition (SVD) factor analysis using Olis GlobalWorks™. Three kinetic species were chosen from the significant eigenvectors resulting from the SVD process and are shown (*left*). The data were fit to an A(blue)→B(dashed line)→C(red) model with the relative amounts of intermediate species with respect to time shown (*right*). Each step was treated as a first order reaction with the following rate constants k_1 = 5.1 x 10^{-1} s^{-1} and k_2 = 5.1 x 10^{-1} s^{-1}.